

## Controlling quasiperiodicity in a CO<sub>2</sub> laser with delayed feedback

A. Labate, M. Ciofini, and R. Meucci

*Istituto Nazionale di Ottica, Largo Enrico Fermi 6, 50125 Florence, Italy*

(Received 24 November 1997)

In this paper we present an experimental scheme for controlling the chaotic regime, reached through quasiperiodicity, of a CO<sub>2</sub> laser with delayed electro-optic feedback. This method, based on a selective filter rejecting one of the two characteristic frequencies of the quasiperiodic motion, allows stabilization of the limit cycle present at the beginning of the bifurcation sequence. By coupling the CO<sub>2</sub> laser model with the differential equations of the filter, we obtain numerical results in good agreement with the experimental observations. [S1063-651X(98)11204-7]

PACS number(s): 05.45.+b, 42.50.Lc, 42.55.Lt

### INTRODUCTION

Dissipative delayed dynamics offers a rich variety of phenomena, specific to high-dimensional systems [1,2]. Such systems are described by means of a delay-differential equation of the type

$$\dot{x} = -\gamma x + F(x(t-\tau)), \quad (1)$$

where  $x(t-\tau)$  is the delayed variable,  $\tau$  is the delay time, and  $\gamma$  accounts for dissipative effects. Paradigmatic examples of delayed dynamics are provided by the Ikeda model for optical turbulence in nonlinear optical resonators [3,4] and by the Mackey-Glass model for physiological control systems [5]. The presence of a delay relates the dynamical variable to a continuous set of initial conditions, and thus the solutions of problem (1) should be found in an infinite-dimensional phase space. However, it was demonstrated by Mallet-Paret that the effective dimension of the attractor is finite [6].

An attractive experimental realization of dissipative delayed dynamics is given by a CO<sub>2</sub> laser, where the output intensity is fed back to an intracavity modulator, eventually with a certain time delay. On the one hand, even for zero delay, the dynamics involves a sufficient number of degrees of freedom [7], so that, for suitable parameter values, the system presents regular or chaotic oscillations. On the other hand, for delays long with respect to the natural period of oscillation, it is possible to find evidence of high-dimensional chaos with intrinsic features similar to those of spatially extended systems, such as defect-mediated turbulence and phase turbulence [8,9]. These analogies have been noted by using a space-time representation for the unidimensional laser signal  $x(t)$  rearranged as a two-dimensional pattern [10]. In the intermediate condition, when the delay is of the same order of the oscillating period, the dynamics becomes low dimensional with evidence of the transition to chaos through quasiperiodicity [11–13]. In this case [14], the two frequencies  $f_1$  and  $f_2$ , induced by the delay time and by the intrinsic feedback mechanism, respectively, compete with each other, determining quasiperiodicity, chaos, and frequency locking.

The aim of the present work is to realize a control scheme suitable for the case of the quasiperiodic route to chaos just

described. Indeed, in the last few years the problem of controlling unstable motion received a large interest, originated by the observations that several unstable periodic orbits are embedded in chaotic attractors, and that small and suitable perturbations allow their stabilization. Ott, Grebogi, and Yorke (OGY) [15] proposed a general feedback method which involves small time-dependent perturbations of a control parameter using appropriate Poincaré sections of the motion in phase space. This method has been successfully applied to experimental systems characterized by slow dynamics, such as the magnetoelastic ribbon [16], chemical reactions [17], and biological systems [18]. In the field of laser physics, the occasional proportional feedback (OPF) method [19], derived from the OGY scheme, has been applied to stabilize periodic orbits and steady states of a chaotic multimode Nd:YAG (yttrium aluminum garnet) laser with an intracavity doubling crystal [20].

Unlike the OGY method, where perturbations are discrete in time, an alternative strategy was introduced by Pyragas [21], based on a continuous feedback with a delay time equal to the period of the unstable orbit to be stabilized. Also, for this method, several experimental implementations have been achieved in laser physics [22,23] and electronic circuits [24].

The control method proposed in the present work differs from both the above schemes, and a detailed comparison with the control strategy introduced by Pyragas was reported in Refs. [25–28] for a chaotic CO<sub>2</sub> laser. Our method involves a frequency domain approach, based on a selective filtering feedback which allows rejection of one of the two competing frequencies. As a consequence the controlled motion is constrained over the limit cycle which precedes the transition to quasiperiodicity.

The importance of this application relies on the fact that the quasiperiodicity route to chaos has been found in many different areas, such as fluid turbulence [29–31], nematic liquid crystals [32], semiconductor lasers with external cavity [23,33], and Langmuir turbulence governed by the Zakharov equations in plasma instabilities [34]. Recently, quasiperiodicity and chaos have also been reported in cardiac fibrillation by Garfinkel *et al.* [35]. In this work experimental data on ventricular tissues suggest that cardiac fibrillation is a form of spatiotemporal chaos arising via a quasiperiodic transition.

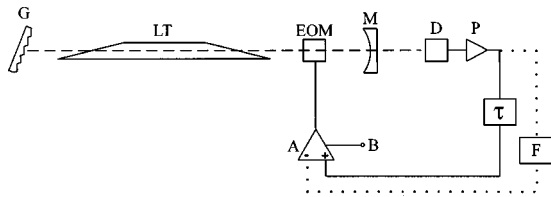


FIG. 1. Experimental setup. *G*, diffraction grating; *LT*, laser tube; *EOM*, electro-optic modulator; *M*, outcoupling mirror; *D*, HgCdTe detector; *P*, preamplifier; *A*, differential amplifier; *B*, bias input;  $\tau$ , delay line. The dotted line represents the control feedback loop containing the selective filter *F*.

### EXPERIMENTAL SETUP AND RESULTS

The experimental setup consists of a single-mode CO<sub>2</sub> laser with a feedback on the cavity losses, realized via an intracavity electro-optic modulator, driven by a signal proportional to the output laser intensity. The experimental setup is described in Fig. 1; the bias voltage *B*, provided by a high-voltage amplifier, is the control parameter of the system. With respect to the experiment of Ref. [28], a delay  $\tau = 6.5 \mu\text{s}$  has been inserted in the feedback loop by using an analog delay line after the first amplification stage. At variance with the case of the laser without delay, the frequency  $f_1$  of the limit cycle established after the Hopf bifurcation ( $B \geq 355 \text{ V}$ ), is related to  $\tau$ . In particular, the oscillation period ( $\sim 13 \mu\text{s}$ ) results in twice the delay time. By increasing

the control parameter *B*, the limit cycle loses its stability at  $B = 565 \text{ V}$ , and we observe the appearance of a two-dimensional torus with a second frequency  $f_2$ ; the ratio  $f_1/f_2$  (winding number) is irrational. A further increase of *B* leads first to the breaking of the torus, and then to a frequency locking regime for  $B \geq 590 \text{ V}$ . In Figs. 2(a)–2(d), we report the reconstruction of the attractors for increasing values of *B*. We will provide subsequently a better evidence of the phenomenon of torus breaking [Fig. 2(c)] by means of Poincaré sections.

It is interesting to characterize the above transitions by a spectral analysis of the temporal signals, with results fundamental to an implementation of our control strategy. We note that the limit cycle behavior [ $B = 565 \text{ V}$ ; Fig. 3(a)] is characterized by a sharp peak at  $f_1 = 73.5 \text{ kHz}$ . The power spectrum of the quasiperiodic motion [ $B = 572 \text{ V}$ ; Fig. 3(b)] presents the emergence of a second principal peak at  $f_2 = 11.6 \text{ kHz}$ , and it also shows a series of secondary peaks due to the combination of the two principal frequencies; the ratio  $f_1/f_2$  is irrational. The situation drastically changes if we further increase the value of *B*. For  $B \geq 590 \text{ V}$  the spectrum still shows the two principal frequencies and their combinations [Fig. 3(c)], but this time the ratio  $f_1/f_2$  is 7. This behavior corresponds to the locking of the two frequencies, also visible on the attractor of Fig. 2(d).

In order to avoid quasiperiodicity, and extend the stability domain of the limit cycle, we introduce a second negative

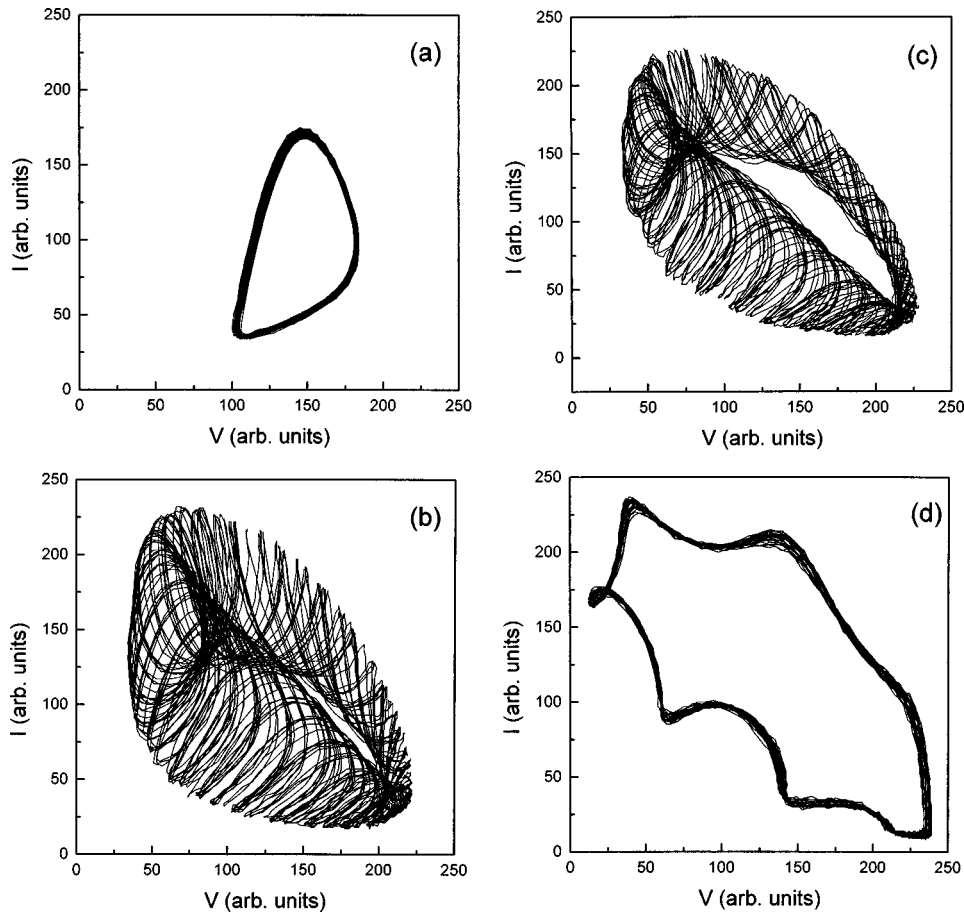


FIG. 2. Experimental phase space plots (laser intensity *I* vs feedback voltage *V*) for the unperturbed dynamics. (a) Limit cycle ( $B = 565 \text{ V}$ ). (b) 2D torus ( $B = 572 \text{ V}$ ). (c) Torus breaking ( $B = 576 \text{ V}$ ). (d) Locking ( $B = 591 \text{ V}$ ).

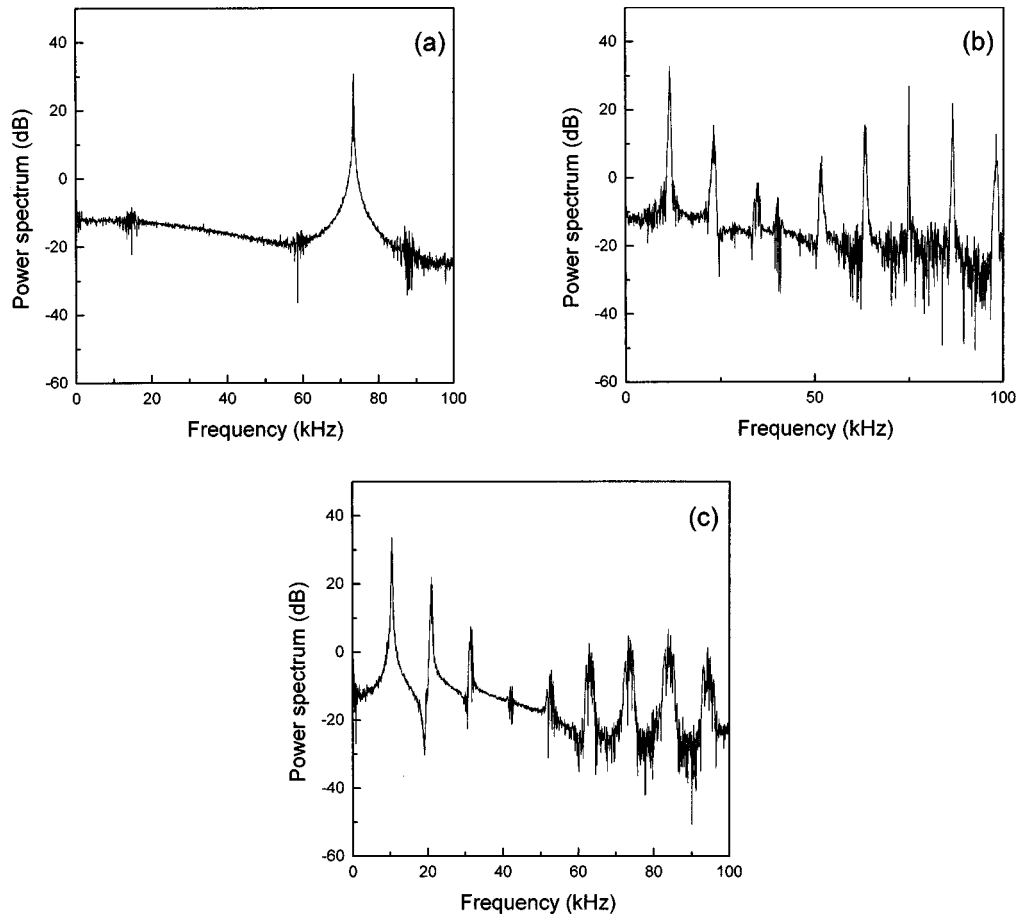


FIG. 3. Experimental power spectra for the unperturbed dynamics. (a) Limit cycle ( $B=565$  V). (b) 2D torus ( $B=572$  V). (c) Locking ( $B=591$  V).

feedback loop which realizes a selective filtering of the undesired lower frequency  $f_2$  (see block  $F$  in Fig. 1). The electrical scheme of the filter is reported in Fig. 4(a), and the transfer function is given by

$$\frac{\nu_0}{\nu_1} = \frac{i\omega L_1 R_2 (1 - \omega^2 L_2 C_2)}{[R_1(1 - \omega^2 L_1 C_1) + i\omega L_1][R_2(1 - \omega^2 L_2 C_2) + i\omega L_2] + i\omega L_1 R_1(1 - \omega^2 L_2 C_2)}. \quad (2)$$

The amplitude response curve [Fig. 4(b)] presents two zeros, one at zero frequency and the other at  $f_1 = 1/2\pi\sqrt{L_2 C_2}$ . On the other hand, the amplitude presents a maximum at  $f_2$ , and the corresponding phase [Fig. 4(c)] is zero. This means that when the filter is inserted in a negative feedback loop, the  $f_2$  component is strongly rejected, thus preventing the transition to the quasiperiodic regime and extending the stability domain of the periodic motion on the limit cycle.

In Fig. 5(a), it is shown the attractor obtained by applying the control signal to the negative input of the high-voltage differential amplifier for  $B=576$  V (torus breaking). The result is a cycle nearly identical to the unperturbed limit cycle. The corresponding power spectrum [Fig. 5(b)] clearly shows that only the  $f_1$  component is still present after the control insertion. Maintaining the same gain in the control loop, the stabilization of the limit cycle is held up to the frequency locking region.

The quasiperiodic regime and the stabilization of the limit cycle can also be usefully represented in terms of Poincaré

maps. In Fig. 6, we show a superposition of the maps corresponding to the different values of  $B$ , together with that corresponding to the stabilized cycle. The maps have been obtained by plotting a maximum of the intensity signal versus the previous one. If a trajectory is sampled by sectioning it with a plane transverse to one of the cyclic coordinates, the result is an infinite set of points that precess around a closed curve, when the behavior is a two-dimensional torus. Then the ringlike structure is a typical signature of a quasiperiodic regime. If the behavior is periodic, the map will be a discrete set of points as for the frequency locking regime, or a single point for the limit cycle. When the quasiperiodicity evolves toward chaos, the ringlike structure will thicken and break, just as in Fig. 6 for  $B=576$  V. It is also important to note that the maps of the unperturbed limit cycle and that of the stabilized cycle are practically coincident, thus confirming the efficacy of our control method; the small difference is related to the fact that the control signal does not vanish when the stabilized orbit has been reached. In order to esti-

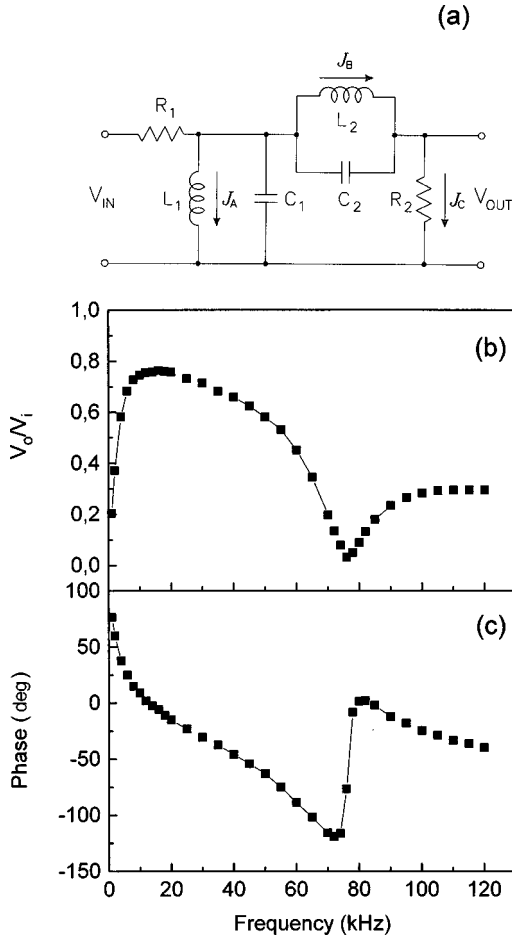


FIG. 4. (a) Electronic scheme of the filter.  $R_1=300\ \Omega$ ,  $L_1=10\ \text{mH}$ ,  $C_1=12\ \text{nF}$ ,  $R_2=1\ \text{k}\Omega$ ,  $L_2=1\ \text{mH}$ , and  $C_2=4.38\ \text{nF}$ . (b) Amplitude response curve. (c) Phase response curve.

mate the relative perturbation  $\varepsilon$  introduced by the control, we performed a ratio between the amplitudes  $E_-$  and  $E_+$  of the signals at the inputs of the high-voltage amplifier. In the two cases corresponding to Figs. 2(c) and 5(a), we obtained  $\varepsilon=4\%$  and  $1\%$ , respectively.

### MODEL

The CO<sub>2</sub> laser is described by the standard four-level scheme, which consists of five differential equations involving the laser intensity  $I$ , the populations of the lasing levels,  $N_1$  and  $N_2$ , and the global populations of the rotational manifolds,  $M_1$  and  $M_2$  [36]. The electro-optic feedback is described by the voltage  $V$  applied, after a delay time  $\tau$ , to an intracavity electro-optic modulator. The global model for the delayed feedback is:

$$\dot{I} = I[-k(V(t-\tau)) + G(N_2 - N_1)],$$

$$\dot{N}_1 = -(z\gamma_R + \gamma_1)N_1 + G(N_2 - N_1)I + \gamma_R M_1,$$

$$\dot{N}_2 = -(z\gamma_R + \gamma_2)N_2 - G(N_2 - N_1)I + \gamma_R M_2 + \gamma_2 P,$$

$$\dot{M}_1 = -(\gamma_R + \gamma_1)M_1 + z\gamma_R N_1,$$

$$\dot{M}_2 = -(\gamma_R + \gamma_2)M_2 + z\gamma_R N_2 + z\gamma_2 P,$$

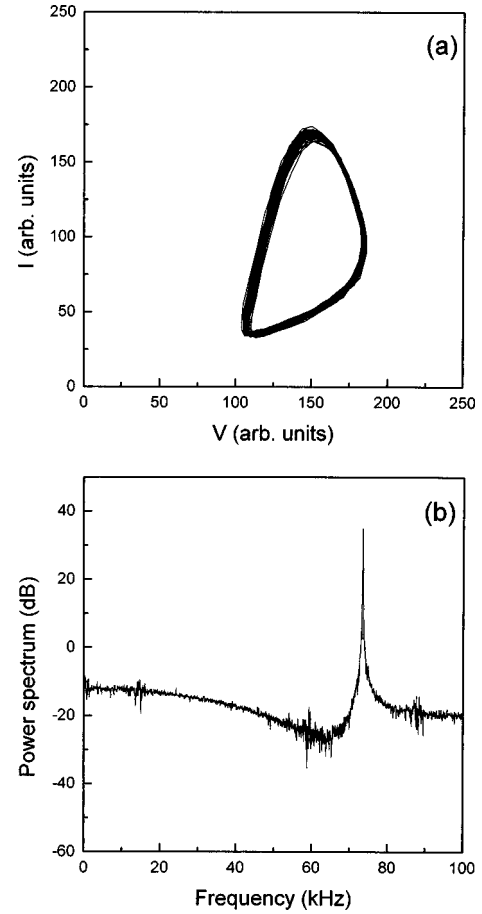


FIG. 5. (a) Experimental phase space plot of the stabilized limit cycle ( $B=576\ \text{V}$ ). The stabilization of the limit cycle is maintained up to the frequency locking condition. (b) Corresponding power spectrum.

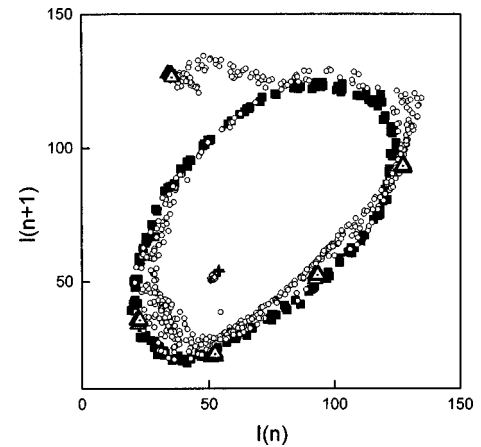


FIG. 6. Poincaré maps of the experimental results. (a) Open diamonds: unperturbed limit cycle ( $B=565\ \text{V}$ ). (b) Solid squares: 2D torus ( $B=572\ \text{V}$ ). (c) Open circles: torus breaking ( $B=576\ \text{V}$ ). (d) Open triangles with dot center: locking ( $B=591\ \text{V}$ ). (e) Crosses: stabilized limit cycle ( $B=576\ \text{V}$ ).

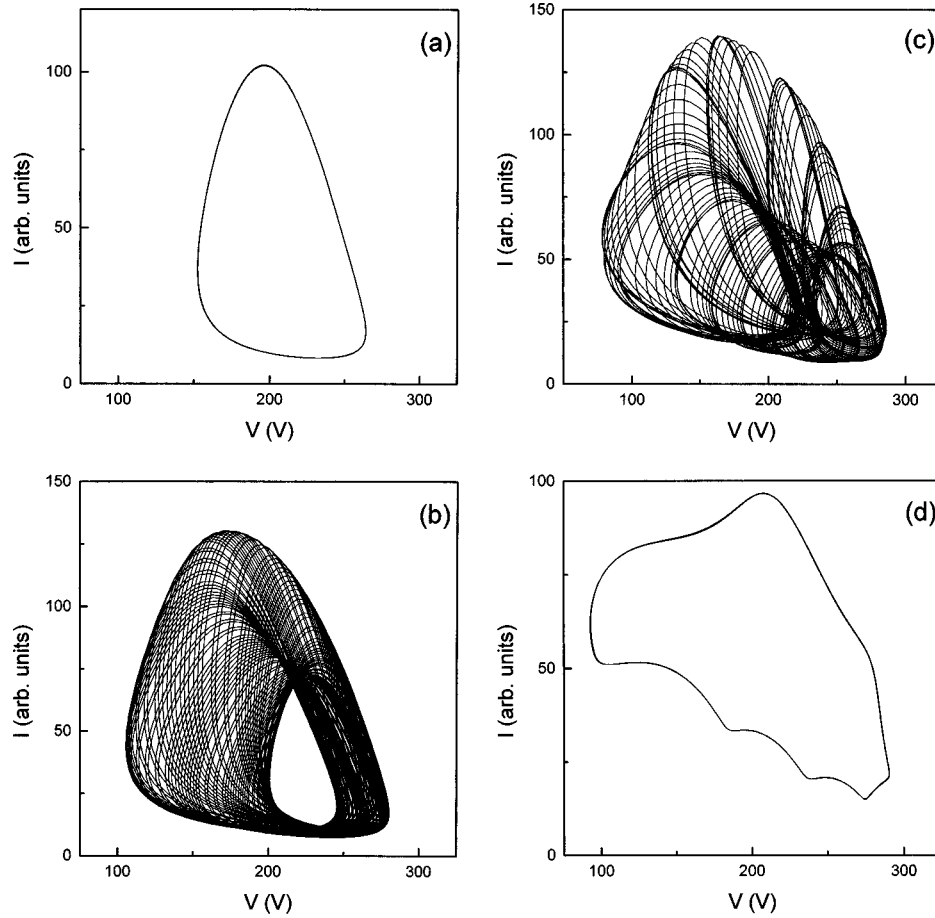


FIG. 7. Numerical results. Phase space plots (laser intensity  $I$  vs feedback voltage  $V$ ) for the unperturbed dynamics. (a) Limit cycle ( $B=334$  V). (b) 2D torus ( $B=335.5$  V). (c) Torus breaking ( $B=336$  V). (d) Locking ( $B=336.2$  V).

$$\dot{V} = -\beta \left( V - B + \frac{RI}{1 + \alpha I} \right). \quad (3)$$

The intensity decay rate  $k$  of the cavity depends on  $V$  as

$$k(V) = k_0 \left[ 1 + k_1 \sin^2 \left( \frac{\pi(V - V_0)}{V_\lambda} \right) \right], \quad (4)$$

where  $k_0 = cT/L$  ( $L=1.35$  m is the cavity length, and  $T=0.09$  is the total transmission coefficient for a single pass),  $k_1 = (1-2T)/2T$ ,  $V_\lambda = 4240$  V is the half-wave voltage of the modulator, and  $V_0 = 100$  V an offset accounting for a small misalignment between the optical axis of the modulator crystal and the polarization direction imposed by the Brewster windows.  $\tau = 6.5 \mu\text{s}$  is the delay inserted in the feedback loop,  $G = 7.3 \times 10^{-8} \text{ s}^{-1}$  is the field-matter coupling constant,  $\gamma_R = 7.0 \times 10^5 \text{ s}^{-1}$  is the relaxation rate between the lasing states and the associated rotational manifolds (the enhancement factor  $z=10$  represents the number of sublevels considered in each manifold),  $\gamma_1 = 8.0 \times 10^4 \text{ s}^{-1}$  and  $\gamma_2 = 1.0 \times 10^4 \text{ s}^{-1}$  are the relaxation rates of the vibrational states, and the adimensional parameter  $P = 3.86 \times 10^{14}$  represents the pump.  $\beta = 300 \text{ kHz}$  and  $R = 2.8 \times 10^{-10} \text{ V/s}$  are the damping rate and the total gain of the feedback loop, respectively, while the term  $\alpha I$  ( $\alpha = 1.2 \times 10^{-13}$ ) takes into account the nonlinearity of the detection apparatus. Once  $P$  and  $R$  are selected, the bias voltage  $B$  acts

as the control parameter. The numerical values of the parameters are deduced from Refs. [28] and [36], except the values of  $P$  and  $R$ , which have been changed due to the different experimental conditions.

Using Eqs. (3) and (4), we can reproduce the observed dynamics, that is the transition from the limit cycle to quasiperiodicity and eventually the torus breaking and locking regime. In Fig. 7 we report the attractors for increasing values of  $B$ . The quasiperiodicity route to chaos is clearly demonstrated by the Poincarè sections of Fig. 8. Comparing the model with the experiment we observe that the two characteristic frequencies of the torus ( $B=335.5$  V) are not exactly reproduced, being  $f_1 = 97.6 \text{ kHz}$  and  $f_2 = 15.9 \text{ kHz}$ . However, the winding number for the locking regime ( $B=336.2$  V) is the same as in the experiment.

The dynamical behavior of our control can be reproduced via differential equations for the electrical currents  $J_A$ ,  $J_B$ , and  $J_C$ , flowing in the branches of  $L_1$ ,  $L_2$ , and  $R_2$ , respectively:

$$R_1 C_1 L_1 \ddot{J}_A + L_1 \dot{J}_A + R_1 J_A = v_i - R_1 J_C,$$

$$R_2 C_2 \dot{J}_C = C_2 L_1 \ddot{J}_A - J_C + J_B,$$

$$C_2 L_2 \ddot{J}_B = J_C - J_B, \quad (5)$$

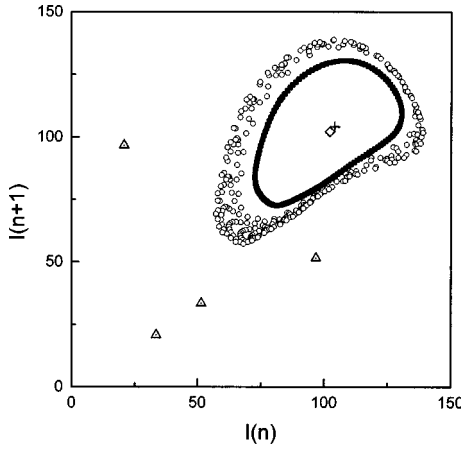


FIG. 8. Poincaré maps of the numerical results. (a) Open diamonds: unperturbed limit cycle ( $B=334$  V). (b) Solid squares: 2D torus ( $B=335.5$  V). (c) Open circles: torus breaking ( $B=336$  V). (d) Open triangles with dot center: locking ( $B=336.2$  V). (e) Crosses: stabilized limit cycle ( $B=336$  V).

where the input  $v_i$  is proportional to the detector voltage, that is  $v_i = \eta I / (1 + \alpha I)$  ( $\eta = 1.04 \times 10^{-14}$  V). In order to match the new values of  $f_1$  and  $f_2$ , we set  $L_1 = 8$  mH,  $L_2 = 0.8$  mH,  $C_1 = 12$  nF,  $C_2 = 3.32$  nF,  $R_1 = 240$   $\Omega$ , and  $R_2 = 1500$   $\Omega$ . Since the filter transfer function is of the fourth order, the above equations can be reduced to a set of four first-order differential equations with output  $v_o = R_2 J_C$ . Consequently, the equation for the feedback voltage in presence of control becomes

$$\dot{V} = -\beta \left( V - B + \frac{RI}{1 + \alpha I} - \mu v_0 \right), \quad (6)$$

where  $\mu = 8.95 \times 10^2$  is the control loop gain.

Figure 9 shows the controlled attractor for  $B = 336$  V, while the corresponding map is superimposed in Fig. 8. In the model, the amplitudes  $E_-$  and  $E_+$  correspond to the last two terms in Eq. (6), so that we have obtained  $E_- / E_+ = 1\%$  without control [Fig. 7(c)], and  $E_- / E_+ = 0.26\%$  with control (Fig. 9). With similar perturbation values, we can obtain stabilization of the limit cycle up to the frequency locking regime.

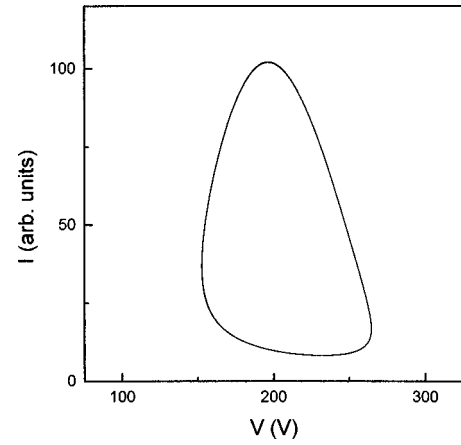


FIG. 9. Numerical result for the stabilized limit cycle ( $B=336$  V), obtained using the filter described by Eqs. (5).

## CONCLUSIONS

In this work we have shown that, in a dissipative system with delayed feedback, the chaotic regime originated by the breaking of a two-dimensional torus can be controlled via a suitable rejection of one of the two fundamental frequencies of the motion. The experimental and theoretical results confirm that the proposed method is rather general, and with a wide range of potential applications, not limited to those dynamical systems where the transition to chaos occurs through a subharmonic bifurcation sequence [26–28]. Possible experimental implementations of our filtering method concern stabilization and control of spatiotemporal structures in optics, as theoretically proposed recently in Refs. [37, 38], or spacelike structures in delayed dynamical systems [39].

## ACKNOWLEDGMENTS

The authors wish to thank F. T. Arecchi and S. Boccaletti (Istituto Nazionale di Ottica), R. Genesio, A. Tesi, and M. Basso (Dipartimento di Sistemi e Informatica of the University of Florence) for useful discussions, and F. Signorini for his contribution of performing the numerical simulations. The work was partly supported by the coordinated project, “Nonlinear dynamics in optical systems” of the Italian National Council of Research, and by EC Contract No. FMRX-CT96-0010 of the project, “Nonlinear Dynamics and Statistical Physics of Spatially Extended Systems.”

- 
- [1] J. D. Farmer, *Physica D* **4**, 366 (1982).
  - [2] K. Ikeda and K. Matsumoto, *J. Stat. Phys.* **44**, 955 (1986).
  - [3] K. Ikeda, *Opt. Commun.* **30**, 257 (1979).
  - [4] K. Ikeda, H. Daido, and O. Akimoto, *Phys. Rev. Lett.* **45**, 709 (1980).
  - [5] M. C. Mackey and L. C. Glass, *Science* **197**, 287 (1977).
  - [6] J. Mallet-Paret, *J. Diff. Eqns.* **22**, 331 (1976).
  - [7] F. T. Arecchi, W. Gadomski, and R. Meucci, *Phys. Rev. A* **34**, 1617 (1996).
  - [8] G. Giacomelli, R. Meucci, A. Politi, and F. T. Arecchi, *Phys. Rev. Lett.* **73**, 1099 (1994).
  - [9] G. Giacomelli and A. Politi, *Phys. Rev. Lett.* **76**, 2686 (1996).
  - [10] F. T. Arecchi, G. Giacomelli, A. Lapucci, and R. Meucci, *Phys. Rev. A* **45**, 4225 (1992).
  - [11] P. Bergé, Y. Pomeau, and C. Vidal, *Order Within Chaos* (Wiley, New York, 1986), Chap. 7.
  - [12] Hao Bai-Lin, *Chaos* (World Scientific, Singapore, 1984), Chap. 7.
  - [13] E. Ott, *Chaos in Dynamical Systems* (Cambridge University Press, Cambridge, 1993), Chap. 6.
  - [14] F. T. Arecchi, G. Giacomelli, A. Lapucci, and R. Meucci, *Phys. Rev. A* **43**, 4997 (1991).
  - [15] E. Ott, C. Grebogi, and J. A. Yorke, *Phys. Rev. Lett.* **64**, 1196 (1990).

- [16] W. L. Ditto, S. N. Rausero, and M. L. Spano, Phys. Rev. Lett. **65**, 3221 (1990).
- [17] B. Peng, V. Petrov, and K. Showalter, J. Chem. Phys. **95**, 4957 (1991).
- [18] A. Garfinkel, M. L. Spano, W. L. Ditto, and J. N. Weiss, Science **257**, 1230 (1992); S. J. Schiff, K. Jerger, D. H. Duong, T. Chang, M. L. Spano, and W. L. Ditto, Nature (London) **370**, 615 (1994); D. J. Cristini and J. J. Collins, Phys. Rev. Lett. **75**, 2782 (1995).
- [19] E. R. Hunt, Phys. Rev. Lett. **67**, 1953 (1991).
- [20] Z. Gills, C. Iwata, R. Roy, I. B. Schwartz, and I. Triandaf, Phys. Rev. Lett. **69**, 3169 (1992).
- [21] K. Pyragas, Phys. Lett. A **170**, 421 (1992); **206**, 323 (1995).
- [22] S. Bielawski, D. Derozier, and P. Glorieux, Phys. Rev. E **49**, R971 (1994).
- [23] C. Simmendinger and O. Hess, Phys. Lett. A **216**, 97 (1996).
- [24] D. W. Sukow, M. E. Bleich, D. J. Gauthier, and J. E. S. Socolar, Chaos **7**, 560 (1997), and references cited therein.
- [25] A. Tesi, E. H. Abed, R. Genesio, and H. O. Wang, Automatica **32**, 1255 (1996); M. Basso, R. Genesio, and A. Tesi, Systems Control Lett. **31**, 287 (1997).
- [26] R. Meucci, M. Ciofini, and R. Abbate, Phys. Rev. E **53**, R5537 (1996).
- [27] M. Ciofini, A. Labate, and R. Meucci, Phys. Lett. A **227**, 31 (1997).
- [28] R. Meucci, A. Labate, and M. Ciofini, Phys. Rev. E **56**, 2829 (1997).
- [29] A. Brandstater and H. L. Swinney, Phys. Rev. A **35**, 2207 (1987).
- [30] M. Dubois, P. Bergé, and V. Croquette, J. Phys. (France) Lett. **43**, 295 (1982).
- [31] J. P. Gollub and H. L. Swinney, Phys. Rev. Lett. **35**, 927 (1975).
- [32] Peng-ye Wang, Jian-hua Dai, and Hong-jun Zhang, Phys. Rev. A **41**, 3250 (1990).
- [33] J. Mork, B. Tromborg, and J. Mark, IEEE J. Quantum Electron. **28**, 93 (1992); A. T. Ryan, G. P. Agrawal, G. R. Gray, and E. C. Gage, *ibid.* **30**, 668 (1994).
- [34] G. I. de Oliveira, F. B. Rizzato, and A. C.-L. Chian, Phys. Rev. E **52**, 2025 (1995).
- [35] A. Garfinkel, Peng-Sheng Chen, D. O. Walter, H. S. Karagueuzian, B. Kogan, S. J. Evans, M. Karpoukhin, Chun Hwang, T. Uchida, M. Gotoh, O. Nwasokwa, P. Sager, and J. N. Weiss, J. Clin. Invest. **99**, 305 (1997).
- [36] A. Varone, A. Politi, and M. Ciofini, Phys. Rev. A **52**, 3176 (1995).
- [37] W. Lu, D. Yu, and R. G. Harrison, Phys. Rev. Lett. **76**, 3316 (1996).
- [38] R. Martin, A. J. Scroggie, G.-L. Oppo, and W. J. Firth, Phys. Rev. Lett. **77**, 4007 (1996).
- [39] S. Boccaletti, D. Maza, H. Mancini, R. Genesio, and F. T. Arecchi, Phys. Rev. Lett. **79**, 5246 (1997).